layers of the dye adsorbed from the high-concentration solutions of the dye resulted in a quantum efficiency of 4.4% based on incident radiation. With the upper bound of absorption by the dye layer being put at 7%, a *lower* bound on the quantum yield for an aggregated adsorbed dye layer is 0.6.

These estimates of the quantum yield in the range 0.6–0.8 confirm our premise that a clean, defect–free electrode surface can serve as an excellent interface for the study of dye-sensitized surfaces. Indirectly, these results support the contention of the literature that surface decomposition products and hydroxide layers can serve as efficient recombination centers in the quenching of dye-sensitized photocurrents at semiconductor electrodes.[2]

In conclusion, with its near ideal behavior, this system should prove useful for modeling the sensitization process. A mathematical treatment for the process using a one-dimensional Onsager model is currently under exploration[14] as is the extension of experimentation to other layered semiconductor/dye systems.

Adsorption of Methoxy on Cu(100)

Daniel Zeroka[†] and Roald Hoffmann*

Department of Chemistry and Materials Science Center, Cornell University, Ithaca, New York 14853

In order to develop a clear understanding of the adsorption of CH$_3$O on metal surfaces we have studied the adsorption of CH$_3$O on the Cu(100) surface since details on the adsorption site preference of CH$_3$O have been recently determined by surface EXAFS. The observed site preference is the 4-fold hollow site with a Cu–O distance of 1.97 Å. Through extended Hückel tight binding solid-state calculations we observe that the main interaction of CH$_3$O with surface copper atoms is through the 2e HOMO level. Effectively no contribution is made by any unoccupied MO due to the high energy of these. This interaction is in marked contrast to CO adsorption where substantial electron density is transferred to the 2π LUMO level. The electron redistribution that occurs on adsorption of CH$_3$O is analyzed through projected density of states diagrams, changes in populations of molecular orbitals and atomic orbitals of the CH$_3$O adsorbate, and changes in electron populations of atomic orbitals of surface atoms.

Introduction

We are interested in the electron redistribution that occurs when methoxy, CH$_3$O, bonds or chemisorbs on a metal surface. Our interest has been triggered by a number of studies. Our original interest was generated from the studies of Ho and co-workers[1] of CH$_3$O on the Ni(110) surface. These studies involved high-resolution electron energy loss spectroscopy (HREELS), time-resolved electron energy loss spectroscopy (TREELS), and thermal desorption spectroscopy (TDS). Subsequent interest followed from several reports[2-4] of the adsorption geometry of CH$_3$O on a Cu(100) surface. Studies[5] related to CH$_3$O on Cu(110) surface are of related interest. At the same time the realization that the reverse process to CH$_3$O adsorption could be an important step in methanol synthesis[6] was another factor in the importance of studying CH$_3$O adsorbed on a metal surface. Indeed there are a plethora of other metal substrates that are candidates for study and whose study would be of interest.

In this report we focus on a highly specific example, the chemisorption of methoxy on a Cu(100) surface. The reason for this choice is that the adsorption geometry of CH$_3$O on this surface was thought to be very well characterized. A recent report[2] of a SEXAFS (surface-extended X-ray absorption fine structure) study indicated

that CH$_3$O bonds oxygen end down in a 4-fold hollow site with a Cu–O distance of 1.97 Å. This adsorption geometry was entirely consistent with a SEXAFS study[7] of O on Cu(100) where the Cu–O distance is 1.94 Å and the oxygen atom adsorbs in a 4-fold hollow site. In addition, vibrational spectra[4a] of surface species indicate that the C–O bond should be upright on the surface.

(1) (a) Richter, L. J.; Gurney, B. A.; Villarrubia, J. S.; Ho, W. *Chem. Phys. Lett.* **1984**, *111*, 185–189. (b) Bare, R. S.; Stroscio, J. A.; Ho, W. *Surf. Sci.* **1985**, *150*, 399–418; **1985**, *155*, L281–L291. (c) Richter, L. J.; Ho, W. *J. Vac. Sci. Technol. A* **1985**, *3*, 1549–1553. (d) Richter, L. J.; Ho, W. *J. Chem. Phys.* **1986**, *83*, 2569–2582.

(2) The following article is concerned with HCO$_2$ adsorbed on Cu(100) but includes the first details of the Cu–O bond distance for CH$_3$O on Cu(100). Stöhr, J.; Outka, D. A.; Madix, R. J.; Döbler, U. *Phys. Rev. Lett.* **1985**, *54*, 1256–1259.

(3) (a) Stöhr, J.; Gland, J. L.; Eberhardt, W.; Outka, D.; Madix, R. J.; Sette, F.; Koestner, R. J.; Doebler, U. *Phys. Rev. Lett.* **1983**, *51*, 2414–2417. (b) Outka, D. A.; Madix, R. J.; Stöhr, J. *Surf. Sci.*, unpublished results.

(4) (a) Sexton, B. *Surf. Sci.* **1980**, *88*, 299–318. (b) Andersson, S.; Persson, M. *Phys. Rev. B* **1981**, *24*, 3659–3662. (c) Ryberg, R. *Chem. Phys. Lett.* **1981**, *83*, 423–426. (d) Ryberg, R. *Phys. Rev. B* **1985**, *31*, 2545–2547. (e) Ryberg, R. *J. Chem. Phys.* **1985**, *82*, 567–573.

(5) (a) Wachs, I. E.; Madix, R. J. *J. Catal.* **1978**, *53*, 208–227. (b) Bowker, M.; Madix, R. J. *Surf. Sci.* **1980**, *95*, 190–206. (c) Carlson, T. A.; Agron, P. A.; Thomas, T. M.; Grimm, F. A. *J. Electron Spectrosc. Relat. Phenom.* **1981**, *23*, 13–24. (d) Sexton, B. A.; Hughes, A. E.; Avery, N. R. *Surf. Sci.* **1985**, *155*, 366–386. (e) Prince, K. C.; Holub-Krappe, E.; Horn, K.; Woodruff, D. P. *Phys. Rev. B* **1985**, *32*, 4249–4251. (f) Bader, M.; Puschmann, A.; Haase, J. *Phys. Rev. B* **1986**, *33*, 7336–7338.

(6) Klier, K. *Adv. Catal.* **1982**, *31*, 243–313.

(7) Döbler, U.; Baberschke, K.; Stöhr, J.; Outka, D. A. *Phys. Rev. B* **1985**, *31*, 2532–2534.

[†] On sabbatical leave for Spring 1985 from the Department of Chemistry, Lehigh University, Bethlehem, PA 18015.

Outka, Madix, and Stöhr in a more recent study[3b] argue that when CH_3O adsorbs on Cu(100) the exact site cannot be determined; however, it is definitely not an on-top site. Interestingly a tilting of the C–O axis of 32° with respect to a surface normal is observed. This tilting is consistent with work of Ryberg,[4c-e] indicating a tilted CH_3O, based on vibrational spectroscopy. Related to the tilting observation it should be noted that recent photoelectron diffraction studies[5e] of CH_3O on Cu(110) indicate two types of adsorbed species—one tilted at 18° in the [1$\bar{1}$0] azimuth and the other tilted by 40° in the [001] azimuth. In this article we focus on the fundamental bonding and orbital interactions of methoxy on Cu(100) without considering a tilted methoxy species on the surface. It is also interesting to note the geometry of CH_3O on Cu(100) in relation to the geometry of CO on the same surface.[8]

## Frontier Orbitals of CH_3O Compared to Those of CO

Not surprisingly, there are substantial differences between the frontier orbitals of CH_3O and CO, and this will result in different bonding to a surface.

For CO the highest occupied MO (HOMO) is 5σ, a lone pair better localized at the C end than at O. This localization, and the consequent better overlap with metal atoms in either discrete transition-metal complexes or on surfaces, is the origin of the preference for the C vs. O bonding. The lowest unoccupied MO (LUMO) is 2π, C–O π antibonding, somewhat more localized on C. It is this orbital, relatively low in energy, which acts as the electron acceptor in CO.

Whereas CO has two π-type orbitals, π (1π, 1) and π^* (2π, 2), OCH_3 has three such orbitals. They may be
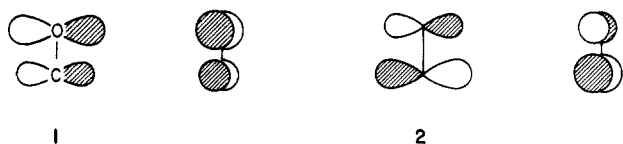
thought of as being derived from the π_{CH_3} and $\pi^*_{CH_3}$ orbitals of a methyl group,[9a] interacting with the π-type lone pair on oxygen, as shown in 3. The crucial orbital 2e is

3
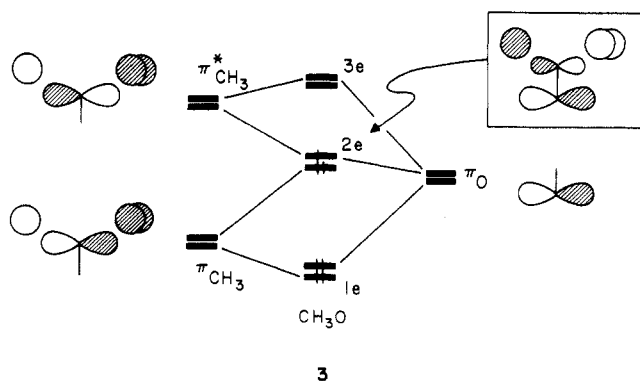
mainly derived from the oxygen π-type lone pair, into which mixes both π_{CH_3} and $\pi^*_{CH_3}$. The interaction with the former dominates, because π_O and π_{CH_3} are close in energy. Thus 2e emerges C–O antibonding, C–H bonding.

At this point we immediately encounter a critical ambiguity in any discussion of the bonding capabilities of

CH_3O whether in an organometallic complex or in adsorption on a surface. Is it better to consider the species adsorbed or bonded as the neutral methoxy radical (three electrons in 2e) or the anionic methoxide anion (2e filled)? To some extent the question is moot: bonded or adsorbed CH_3O is somewhere in between CH_3O and CH_3O^-. If one starts from the neutral fragment, the electron transfer on bonding or chemisorption will be from metal to CH_3O. If one starts from anionic CH_3O^-, the electron drift will be in the opposite direction, to the metal. Nature dictates the exact form of the molecular species bonding to the metal; however, for an electronic structure calculation the question is one of convention and convenience. Here we choose a starting point of CH_3O neutral, three electrons in 2e.

The unfilled orbitals of CH_3O are much higher, relative to the HOMO, than in the case of CO. They are 3e, mainly $\pi^*_{CH_3}$, and $6a_1$, a mixture of $\sigma^*_{CH_3}$ and σ^*_{CO}.

CH_3O Adsorbed on Cu(100) Surface

We now turn to the adsorption of CH_3O on the Cu(100) surface and consider the following fundamental questions: What key electron flow or electron redistribution occurs when CH_3O adsorbs on a particular site of a Cu(100) surface? What differences can be detected when adsorption occurs at different sites? Can we predict site preferences for adsorption and if so what is (are) the key indicator(s) of site preference?

In the analysis that we present here we concentrate on the participation of the frontier orbitals of the adsorbate. Before we get started with the detailed calculation and analysis let us anticipate what results are expected. The LUMO level of CH_3O is computed as energetically very high (difference of 18.7 eV) relative to the HOMO level so that no significant participation of the LUMO level is expected. In addition, since the energy of the HOMO level is –14.2 eV compared to the H_{ii} for the 3d orbitals of copper of –14.0 eV, we expect substantial interaction of CH_3O with the d orbitals of copper. This line of reasoning makes use of the interaction[9b] of two orbitals i and j being given by $H^2_{ij}/(E_j - E_j)$. Since the energy of the HOMO level of CH_3O is somewhat lower than the H_{ii} of copper, we expect electron transfer to occur from the metal to CH_3O; i.e., CH_3O should act as a Lewis acid toward the copper metal surface. Note that this assumes a vacancy in the HOMO of CH_3O, i.e., a convention of a neutral isolated CH_3O fragment.

Now we wish to map out the electron redistribution that occurs upon adsorption. We use the approach previously used by our research group to study adsorption.[10] That approach considers the process of forming an adsorbate on a metal surface from a bare monolayer of adsorbate, in the same orientation under consideration for the surface, and a bare metal slab corresponding to the particular surface of the metal. Symbolically, for our highly specific example,

$$Cu[(100);slab] + CH_3O(monolayer) \rightarrow Cu(100)\cdots CH_3O$$

(1)
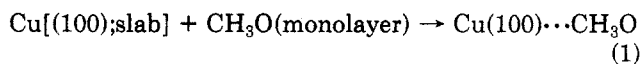
Now some tricky detective work is needed to find in the product or composite electron distribution clues leading us to the important interactions responsible for metal slab–monolayer adsorbate bonding. One technique

(8) (a) Allyn, C. L.; Gustafsson, T.; Plummer, E. W. *Solid State Commun.* **1977**, *24*, 531–537. (b) Andersson, S. *Surf. Sci.* **1979**, *89*, 477–485.

(9) (a) Jørgensen, W. L.; Salem, L. *The Organic Chemists' Book of Orbitals*; Academic Press: New York, 1973; p 8. (b) Hoffmann, R. *Acc. Chem. Res.* **1971**, *4*, 1–9.

(10) (a) Saillard, J.-Y.; Hoffmann, R. *J. Am. Chem. Soc.* **1984**, *106*, 2006–2026. (b) Sung, S.; Hoffmann, R. *J. Am. Chem. Soc.* **1985**, *107*, 578–584. (c) Silvestre, J.; Hoffmann, R. *Langmuir* **1985**, *1*, 621–647. (d) Sung, S.; Hoffmann, R.; Thiel, P. A. *J. Phys. Chem.* **1986**, *90*, 1380–1388.

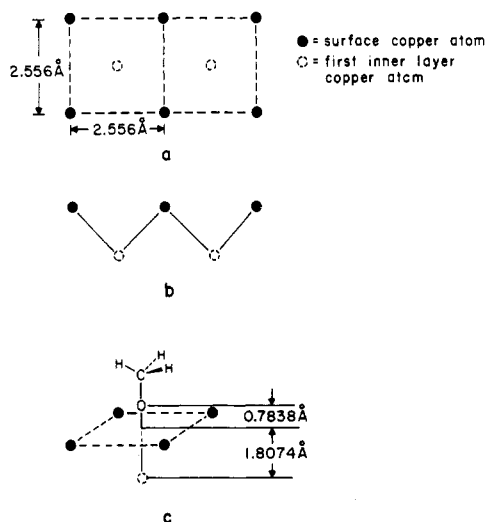**Figure 1.** Geometrical arrangement on surface: (a) View of Cu(100) surface looking along [00Ī] direction. (b) View of Cu(100) surface looking along [010] direction. (c) Adsorption of CH_3O, oxygen end down, on a 4-fold hollow site. Also shown is one of the inner layer copper atoms. The position of the oxygen above the surface is chosen to correspond to the Cu–O distance determined by surface EXAFS.

Table I. Summary of Electron Redistribution That Occurs When CH_3O Adsorbs on Cu(100) Surface[a]

overlap population		
Cu–O	0.17	
O–C	0.57	(0.63, CH_3O monolayer; 0.55, CH_3O^- monolayer)
C–H	0.79	(0.71 CH_3O monolayer; 0.79, CH_3O^- monolayer)
CH_3O MO electron densities		
2e	3.63	(3, CH_3O monolayer)
$6a_1$	0.01	(0, CH_3O monolayer)
electron density changes on surface atoms		
Δs	−0.372	
Δp_σ	0.081	
Δp_π	0.036	
Δd_σ	0.001	
Δd_π	−0.019	
Δd_δ	−0.014	
total	−0.287	
energy change, ΔE	−1.58 eV	
Fermi energy, ϵ_F	−10.23 eV	

[a] The adsorption is set at the experimentally observed 4-fold hollow site with oxygen end down and Cu–O distance of 1.97 Å.

available that we use is a comparison of density of states[11] for each solid.

We look first at adsorption in the experimentally observed 4-fold hollow site. The geometrical structures for the 4-fold hollow site are shown in Figure 1. The methoxy moiety is displaced above the surface plane by 0.7838 Å, to correspond to the Cu–O distance of 1.97 Å observed by surface EXAFS. Other bond distances and bond angles for CH_3O are taken from the study of Gerry, Lees, and Winnewisser.[12] As already mentioned, the reason for study of this surface is the availability of the adsorption geometry. We are not aware, at this time, of other metal surfaces for which the adsorption geometry of CH_3O is available.

In the hypothetical "reaction" that we are considering, we are pushing a monolayer of adsorbate onto a metal slab. First let us consider the metal slab. Previous studies[10] in our research group indicate that a metal surface is reasonably represented by a slab of 3–4 atom thickness; i.e., the inner atom layer has a density of states similar to bulk metal. In this study we use a three-layer slab. For copper, extended Hückel parameters needed are taken from previous work and are summarized in the Appendix. The density of states for the Cu(100) surface is shown in Figure 2a. The d block and part of the s and p block are shown. The energy window used for all density of states drawings is −20 to −8 eV. The s and p blocks, not shown in total, are quite broad with a total width of 14 eV whereas the d block is approximately 2 eV wide. The Fermi level is calculated to be at −10.25 eV.

Now the density of states for a CH_3O monolayer must be determined. In the calculations we report here we will take a coverage of $\theta = 1/2$. At that coverage we must be careful that hydrogen atoms of adjacent CH_3O fragments do not approach each other to a physically unreasonable distance. For this reason we orient the CH_3O's of a monolayer in a way which tends to minimize the H–H overlap for adjacent CH_3O's. The orientation selected has

a C–H bond oriented along the [Ī10] direction. This orientation is shown in 4. The calculated density of states
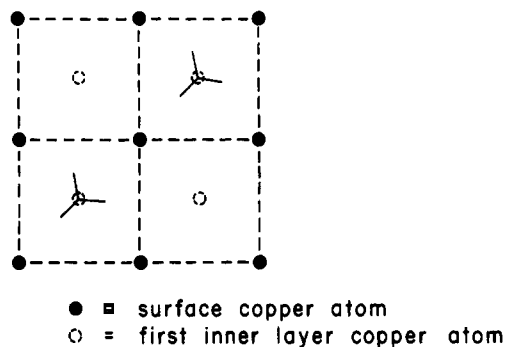
4

is shown in Figure 2c. Note the bands shown in this energy window are formed from the 1e, $5a_1$, and 2e orbitals. The width of the bands is due to the overlap of CH_3O's at the coverage of $1/2$ that we are using. The combined monolayer and metal slab density of states is given in Figure 2b. Clear mixing of the 2e HOMO level of CH_3O with the d block of copper has occurred, as may be seen by comparing the different components of Figure 3. The contribution of each CH_3O molecular orbital can be seen more clearly from analyses of projected density of states. In Figure 3 the contributions of selected molecular orbitals to the total density of states are shown for the 1e, $5a_1$, and 2e orbitals. Clearly, the lower band arises predominantly from the 1e and $5a_1$ states. The 2e HOMO level mixes substantially with the d block of the metal. The $6a_1$ LUMO level, not shown here, mixes with the s and p block of the metal and is clearly lowered in energy from 4 to 0 eV. However, this energy is still substantially above the Fermi level ϵ_F of −10.2 eV. As a consequence, essentially no electron flow into the LUMO level occurs. This nonparticipation of the LUMO level is in marked contrast to CO adsorption, where significant electron density flows into the $2\pi^*$ LUMO level.[10b]

Other indicators of the electron redistribution that has occurred on adsorption are summarized in Table I. First, note that there is surprisingly little change of copper d orbitals on adsorption of CH_3O. On some reflection we observe that the site under consideration is not an on-top site and the diffuse d orbitals will not have strong overlaps

(11) Ashcroft, N. W.; Mermin, N. D. *Solid State Physics*; Saunders: Philadelphia, 1976; pp 44, 143–145.

(12) Gerry, M. C. L.; Lees, R. M.; Winnewisser, G. *J. Mol. Spectrosc.* **1976**, *61*, 231–242.
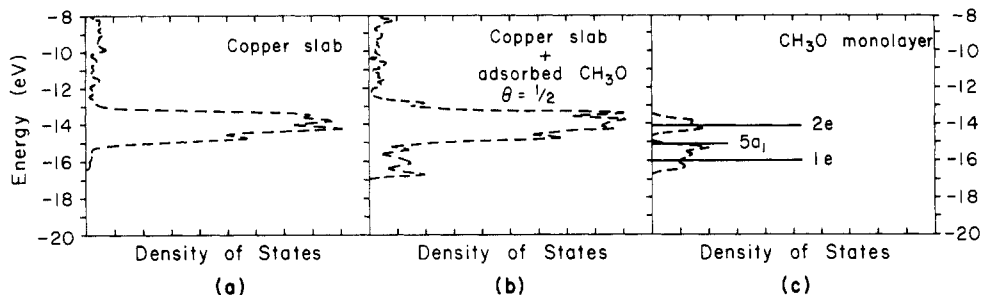
Figure 2. Density of states for the following solids: (a) three-layer copper slab; (b) CH_3O adsorbed with coverage $\theta = {}^1/_2$; (c) CH_3O monolayer. Valence molecular energy levels in the energy window of –20 to –8 eV for free CH_3O are indicated by bars.
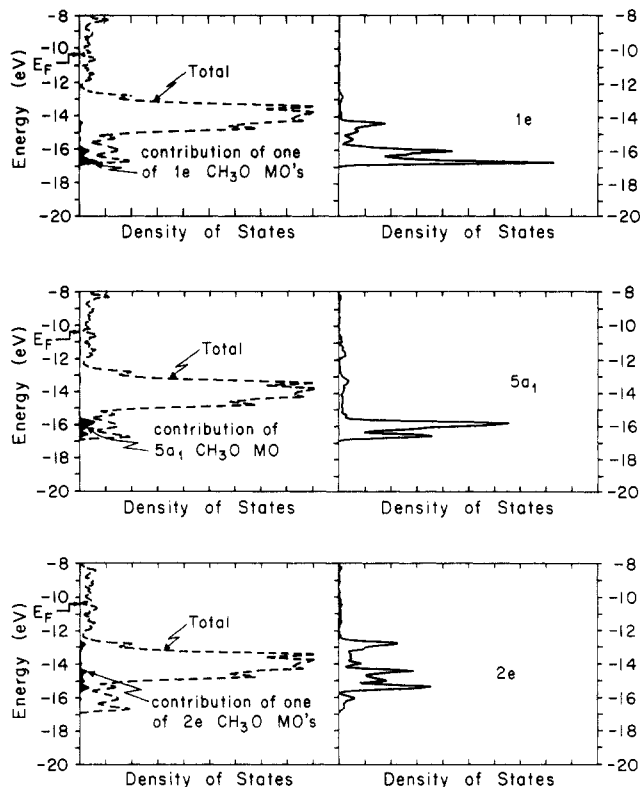

Figure 3. Projected density of states for selected molecular orbitals of CH_3O, when CH_3O is adsorbed in a 4-fold hollow site. These projected density of states give the contribution of each molecular orbital to the total energy of states. The projected density of states for each orbital contribution shown on the left is magnified with a multiplication factor of 11 and the magnification is shown on the right.

with the oxygen atom of the adsorbate. Greater changes are observed to occur in the contribution of metal 4s and 4p. As already mentioned, in the projected density of states plots the $6a_1$ LUMO in effect does not change its occupation whereas the 2e HOMO level mixed substantially with the metal d block. Note the occupation of 2e by 3.63 electrons. We have moved a good part of the way from CH_3O (occupation = 3.0) to CH_3O^- (occupation = 4.0). This is also clear from the C–O and C–H overlap populations which resemble more isolated methoxide anion than radical.

Adsorption at On-Top Site

Can we detect any clear changes that occur when adsorption occurs at a different site? Let's consider adsorption at an on-top site. Since the oxygen atoms of CH_3O would now be 1-fold coordinated to a metal atom as compared to the previous 4-fold coordination it would be expected that the metal–oxygen distance may be

Table II. Summary of Electron Redistribution That Occurs When CH_3O Adsorbs on Cu(100) Surface[a]

overlap populations		
Cu–O	0.23	
O–C	0.55	(0.63, CH_3O monolayer;
		0.55, CH_3O^- monolayer)
C–H	0.79	(0.71, CH_3O monolayer;
		0.79, CH_3O^- monolayer)
CH_3O electron densities		
2e	3.98	(3, CH_3O monolayer)
$6a_1$	0.0022	(0, CH_3O monolayer)
electron density change		
on surface atoms		
Δs	–0.270	
Δp_σ	0.135	
Δp_π	–0.020	
Δd_σ	–0.050	
Δd_π	0.000	
Δd_δ	–0.006	
total	–0.211	
energy change, ΔE	–3.341 eV	
Fermi energy, ϵ_F	–10.70 eV	

[a] The adsorption is set at an on-top site with oxygen end down and Cu–O distance at 1.97 Å.
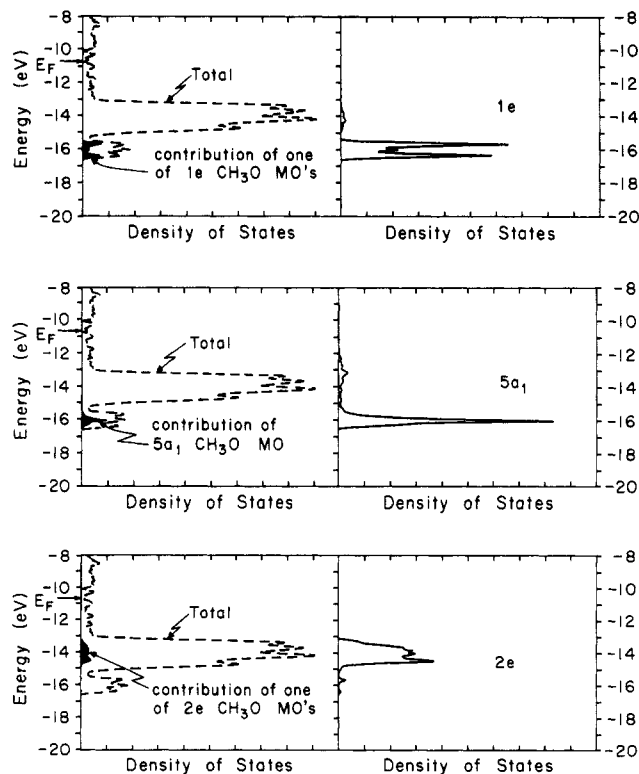

Figure 4. Projected density of states for selected molecular orbitals of CH_3O when CH_3O is adsorbed at an on-top site. The projected density of states for each orbital contribution shown on the left is magnified with a multiplication factor of 8.6 and the magnification is shown on the right.
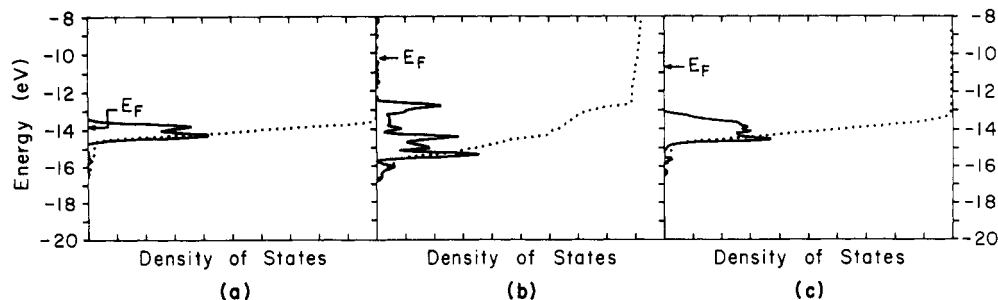
Figure 5. Comparison of projected density of states for the HOMO molecular orbital of CH_3O: (a) CH_3O monolayer; (b) 4-fold hollow site adsorption; (c) on-top site adsorption. The dotted line corresponds to the integrated density of states.
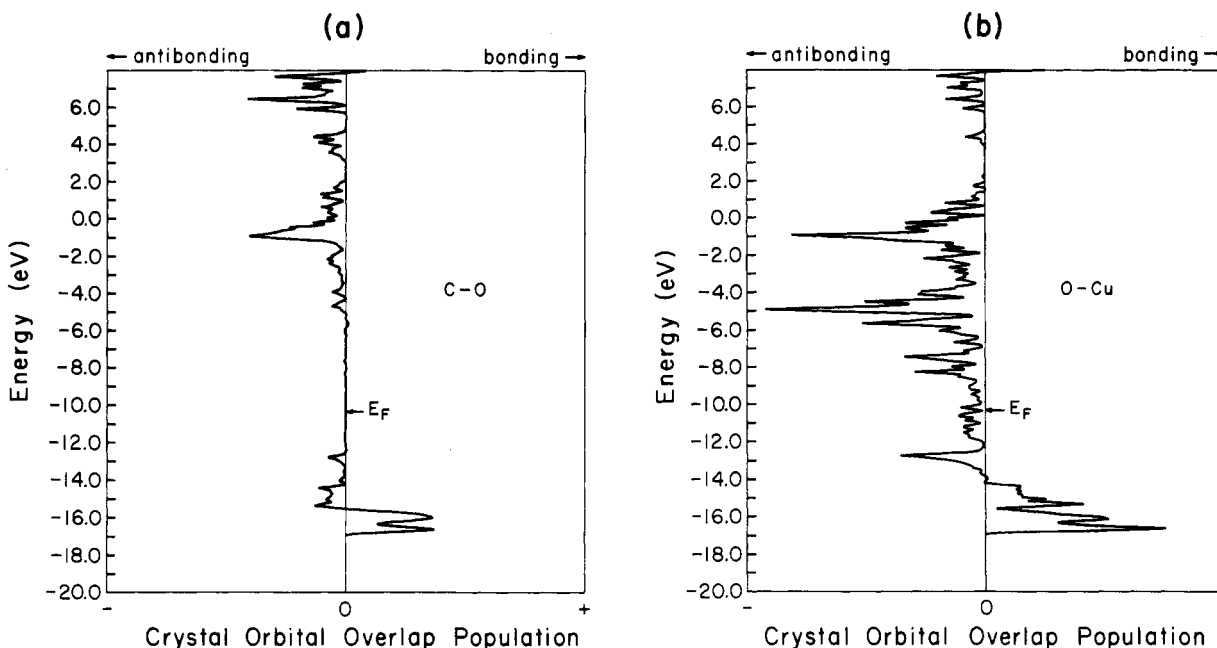
Figure 6. COOP curves for adsorption in a 4-fold site: (a) C–O; (b) O–Cu.

somewhat different. However, for the present calculation let us keep the Cu–O fixed at 1.97 Å. The calculations are summarized in Figures 4 and 5 and Table II. The total density of states for on-top adsorption, which can be seen in Figure 4, is not very different from that for 4-fold co-ordination. Projected densities of states are more informative. The main observation to be made here is that the HOMO level contributes only to the d block, in marked contrast to the HOMO level mixing with not only the d block, but also the s and p blocks in the adsorption in the 4-fold hollow site. The contribution of the HOMO level of CH_3O is perhaps more clearly evident in Figure 5. Here comparison of the contributions of the 2e HOMO level for the CH_3O monolayer, 4-fold hollow site, and on-top site shows the mixing that occurs for the 4-fold hollow site. Also, a comparison can be made of the occupation of the HOMO level of CH_3O.

By noting the Fermi levels reported in Tables I and II and by observing the integrated density of states shown in Figure 5 for the 2e HOMO level, one can readily observe that the 2e HOMO level is essentially completely filled for CH_3O adsorbed in an on-top site with a fractional occu-pation of 0.995 (3.98 electrons out of 4); however, for CH_3O adsorbed in a 4-fold hollow site a fractional occupation of 0.908 (3.63 electrons out of 4) is seen. In Table II electron populations are reported for the on-top site. A few clear differences in the electron populations relative to the 4-fold hollow site, reported in Table I, are observed. In the on-top site there is more electron transfer from Cu. A detailed analysis shows that the transfer is to O of CH_3O and

specifically to oxygen π-type orbitals. But this does not mean more O 2p–Cu 3d interaction, for the Cu $3d_\pi$ occu-pation is unchanged. The electron transfer to oxygen comes in large part from Cu $4p_\pi$, see interaction 5, and also from the copper atoms not involved in adsorbate bonding.

5
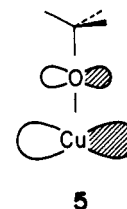
In Figure 6 we make use of another tool for consideration of bonding in the solid state. This is the crystal orbital overlap population,[11a] COOP, or overlap population weighted density of states. The COOP curves for on-top adsorption differ a little in detail but essentially resemble those for 4-fold site adsorption and so are not shown here.

The analysis of the COOP curves is best done in con-junction with looking at the orbital contributions to the total DOS. CO bonding is picked up through 1e but di-minished through occupation of 2e (see **3** for CO anti-bonding nature of 2e). Thus the CO overlap population in adsorbed CH_3O is lower than in free CH_3O. But it is not very different from that in free OCH_3^- or a monolayer of that anion. Clearly the methoxy on the surface has moved closer to methoxide anion in its bonding charac-teristics.

Table III. Extended Hückel Parameters

atom	atomic orbital	H_{ii}, eV	$\zeta_1{}^a$	ζ_2	$c_1{}^a$	c_2
Cu	3d	−14.0	5.95	2.30	0.5933	0.5744
	4s	−11.4	2.20			
	4p	−6.06	2.20			
C	2s	−21.4	1.625			
	2p	−11.4	1.625			
O	2s	−32.3	2.275			
	2p	−14.8	2.275			
H	1s	−13.6	1.3			

^{a} Exponents and coefficients in double-ζ expansion.

Cu–O bonding is picked up in 1e and 2e. But the total Cu–O overlap population is not very large, and this is because Cu–O antibonding states are also occupied. These may be clearly seen around −13 eV in the COOP curves and give evidence for O–Cu d-block interaction, even when such interaction is not easily seen from Cu d orbital occupations.

Let us be a little more specific on this point, because it is an important one. The contribution to the DOS of 2e (Figure 3) shows a small peak at −13 eV, just where the COOP curves show Cu–O antibonding. But the main part of the 2e is at −14.5 to −16.5 eV. A representative orbital of the lower part is 6; one of the upper part is 7. Both are filled, so both 2e and Cu d_π are filled. But the COOP curve gives evidence of their interaction.
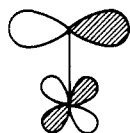

6
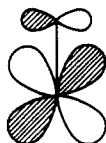
7

Comments and Discussion

In order to follow the electron redistribution that occurs when CH_3O adsorbs on a Cu(100) surface, we have used the tools of solid-state chemistry presently available, those tools being density of states, projected density of states, electron populations, and COOP curves. Our main observation is that the dominant interaction of CH_3O with the surface is through the HOMO level of CH_3O with the d block of the metal. Since no electron transfer to the

LUMO level occurs for CH_3O, no C–O bond weakening follows because of that transfer. However, some weakening of the C–O bond does arise as the HOMO level population increases, since this level is C–O antibonding. The bond weakening that occurs apparently is not sufficient to break the C–O bond relative to abstraction of one of the H atoms by metal atoms on the surface. Chemisorbed methoxy, $CH_3O(a)$, is observed to primarily desorb as molecular formaldehyde according to the mechanism

$$CH_3O(a) \rightarrow CH_2O(a) + H(a) \rightarrow CH_2O(g)$$
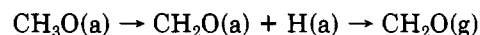
where adsorbed formaldehyde, $CH_2O(a)$, has not yet been experimentally detected.[1–4,13] In addition chemisorbed methoxy is observed to form formate, HCOO, in small amounts due presumably to the reaction with adsorbed oxygen, present as a contaminant, as

$$CH_3O(a) + O(a) \rightarrow HCOO(a) + 2H(a)$$
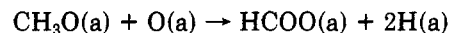
The H abstraction involved in the formation of formaldehyde is of interest and will be considered in another study, presently in progress, of CH_3O adsorbed on the Ni(110) surface. In that study, posible tilting of the CH_3O on the surface is taken into account as a step before cleavage of one of the C–H bonds.

Appendix

The extended Hückel method,[14a] with weighted H_{ij}'s,[14b] in a tight-binding band implementation[14c,d] was used. The parameters are listed in Table III.

Registry No. CH_3O, 2143-68-2; Cu, 7440-50-8.

(13) Richter, L. J., private communication.

(14) (a) Hoffmann, R. *J. Chem. Phys.* **1953**, *39*, 1397–1413. Hoffmann, R.; Lipscomb, W. N. *Ibid.* **1962**, *36*, 2179–2189, 3489–3493; **1962**, *37*, 2872–2883. (b) Ammeter, J. H.; Bürgi, H.-B.; Thibeault, J. C.; Hoffmann, R. *J. Am. Chem. Soc.* **1978**, *100*, 3686–3692. (c) Whangbo, M.-H.; Hoffmann, R. *J. Am. Chem. Soc.* **1978**, *100*, 6093–6098. (d) Whangbo, M.-H.; Hoffmann, R.; Woodward, R. B. *Proc. R. Soc. London, Ser. A* **1979**, *A366*, 23–46.